

Measurements of Equilibria and Reactivity of Cluster Ions at Atmospheric Pressure: Reactions of $\text{Cl}^-(\text{CHCl}_3)_{0-2}$ with CH_3Br and CH_3I

K. Giles and E. P. Grimsrud*

Department of Chemistry, Montana State University, Bozeman, Montana 59717

Received: August 18, 1992; In Final Form: November 23, 1992

Measurements by the kinetic ion mobility mass spectrometer (KIMMS) of (i) equilibrium constants for the clustering reactions $\text{X}^-(\text{CHCl}_3)_{i-1} + \text{CHCl}_3 \rightleftharpoons \text{X}^-(\text{CHCl}_3)_i$, where $\text{X}^- = \text{Cl}^-$ and Br^- and $i = 1$ or 2 , (ii) single ion mobilities for the ions $\text{Cl}^-(\text{CHCl}_3)_{0-2}$ and $\text{Br}^-(\text{CHCl}_3)_{0-1}$, and (iii) rate constants for the $\text{S}_{\text{N}}2$ nucleophilic displacement reactions of a distribution of chloride cluster ions, $\text{Cl}^-(\text{CHCl}_3)_{0-2}$, with CH_3Br and with CH_3I in nitrogen buffer gas at atmospheric pressure are reported. A unique feature of the present equilibrium and kinetic measurements is that they are obtained from ion mobility measurements and, therefore, are not subject to potential sources of error that can accompany mass spectrometric-based measurements involving aperture sampling of a high-pressure ion source. Another unique feature of the present investigation is that the reactivity of a selected set of cluster ions is determined under physical conditions in which the individual ions are kinetically labile with respect to cluster decomposition and growth.

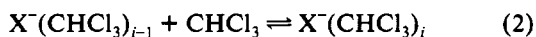
Introduction

Very few measurements of ion–molecule reactions have been reported, to date, using buffer gas pressures exceeding a few Torr,^{1–6} in spite of the fact that interesting effects can be anticipated with the use of higher pressures.^{7,8} In a recent contribution to this journal,⁹ we described the kinetic ion mobility mass spectrometer (KIMMS), which was designed specifically for the study of ion–molecule reactions in a buffer gas of 1 atm of pressure. In our initial report of the KIMMS, it was demonstrated that rate constants for ion–molecule reactions at atmospheric pressure could be determined to a level of accuracy (about $\pm 20\%$) that compares favorably to that obtained by the well-established methods that operate at much lower pressures. An interesting effect of elevated pressure was revealed in the initial study. It was found that the rate constant for the $\text{S}_{\text{N}}2$ nucleophilic displacement reaction



was significantly greater in atmospheric pressure nitrogen buffer gas relative to that reported in methane buffer gas at 4 Torr. This pressure dependence for reaction 1 is thought to reflect the importance of increased collisional stabilization at atmospheric pressure of a short-lived intermediate along the $\text{S}_{\text{N}}2$ reaction pathway of this reaction.

With use of an atmospheric pressure buffer gas, the partial pressure of a neutral clustering agent can be made relatively high so that the formation of cluster ions is facilitated. It is therefore anticipated that the KIMMS instrument will be particularly useful for the study of ion–molecule reactions involving clustered ions and its first application for this purpose is reported here. Specifically, it will be shown that equilibrium constants for halide ion–chloroform clustering reactions

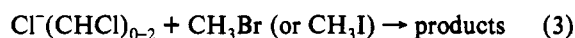


where $\text{X}^- = \text{Cl}^-$ or Br^- and $i = 1$ or 2 , can be determined by measurements of ion mobility as a function of the concentration of CHCl_3 added to the drift gas. An attractive feature of this approach to cluster equilibrium measurements is that it is not subject to the potential sources of measurement error (aperture perturbations and detection mass bias effects) that are commonly associated with mass spectrometric-based methods.^{10–13} It will also be shown that the mobilities of individual halide–chloroform cluster ions can be determined by these measurements. Finally,

TABLE I: Typical Conditions of the KIMMS

drift gas/flow rate	$\text{N}_2/525 (\pm 13) \text{ cm}^3 \text{ min}^{-1}$
source gas/flow rate	$\text{N}_2/50 (\pm 5) \text{ cm}^3 \text{ min}^{-1}$
temperature	$75\text{--}125 (\pm 5) \text{ }^\circ\text{C}$
pressure	$640 (\pm 10) \text{ Torr}$
drift field strength	140 V cm^{-1}
drift field length	23.7 cm
Tyndall gate pulse width	0.2 ms
sweeps per ion mobility spectrum	500
sweeps per mass-analyzed IM spectrum	5000

it will be shown that rate constants for the reactions of any selected set of equilibrated chloride–chloroform cluster ions with methyl bromide or methyl iodide (reaction 3) can be determined under



physical conditions in which the reagent cluster ions are kinetically labile with respect to decomposition or growth by reaction 2.

Experimental Section

The KIMMS instrument has recently been described in detail,⁹ and only a summary of its operating principles will be provided here. A summary of the typical operating conditions for the present study is provided in Table I. Cl^- or Br^- ions are initially produced in a ^{63}Ni ion source by electron capture to either CCl_4 or CF_3Br , respectively, which are added in small quantities to the source gas (nitrogen, atmospheric pressure). A Tyndall ion gate allows the source ions to enter a drift region either continuously or in short pulses. In the drift region, ions are transported through nitrogen gas at atmospheric pressure to a Faraday plate at a rate determined by their respective mobilities. During transport through the drift region, the ions can undergo ion–molecule reactions with neutrals added to the drift gas. When relatively large amounts of CHCl_3 are added to the drift gas, an equilibrium condition for reaction 2 will be quickly established at all points along the drift tube. When small amounts of CH_3Br are also added to the drift gas, reaction 3 is expected to also occur at a slower rate along the length of the drift tube. Since the ratio of the drift field (140 V/cm) to the pressure is very low, the internal energy of the ions is not significantly affected by the drift field.⁹ Therefore, the equilibrium and kinetic measurements reported here can be considered to reflect the reactions of thermalized, rather than excited, reagent ions. Measurements of ion arrival at the Faraday plate are made both by an electrometer connected

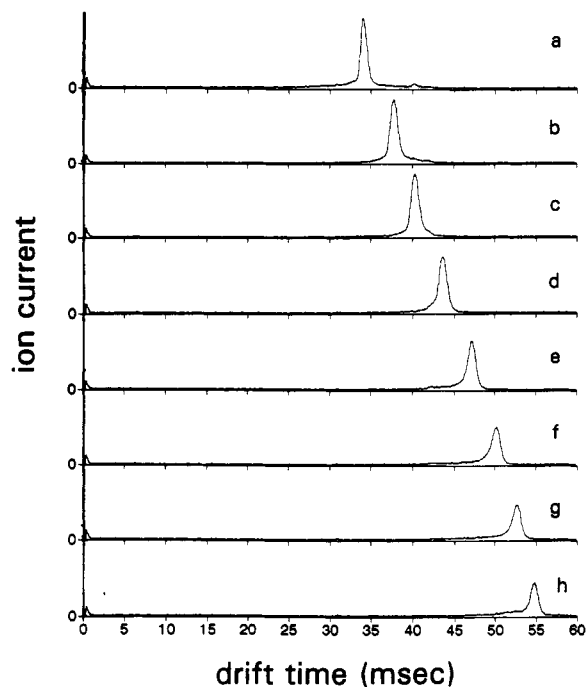


Figure 1. Ion mobility spectra obtained by the production of Cl^- by electron capture to CCl_4 in the ion source with the following partial pressures of CHCl_3 added to the drift gas: (a) none, (b) 1.61×10^{-6} , (c) 3.2×10^{-6} , (d) 6.5×10^{-6} , (e) 1.29×10^{-5} , (f) 2.6×10^{-5} , (g) 5.2×10^{-5} , and (h) 1.03×10^{-4} atm. Ion source and drift regions contain nitrogen buffer gas at 640 Torr and 125 °C. Tyndall gate pulse width is 0.2 ms. Each spectrum shown is the average of 500 scans. The full scale range for each spectrum is 0.050 nA.

to the plate and by an associated mass spectrometer that samples the contents of gas leaking through a 50- μm aperture located at the center of the Faraday plate. The Faraday plate electrometer thereby provides a "total" ion mobility spectrum, and the mass spectrometer provides a "single" ion mobility spectrum of any mass-selected ion of interest. The mass spectrometer also provides an alternate means of measuring reaction rates under conditions in which the Tyndall gate is left continuously open.

Results and Discussion

Ion Cluster Equilibria and Mobilities. In Figure 1, a series of mobility spectra recorded by the Faraday plate electrometer are shown under conditions in which Cl^- has been produced by electron capture to CCl_4 in the ion source and various amounts of CHCl_3 have been added to the drift gas. It is seen that the arrival time of the major ion signal increases with increasing concentration of CHCl_3 . In Figure 2, a mass spectrum (obtained with the Tyndall gate set continuously open) is shown to include four different chloride-containing ions under conditions of relatively high CHCl_3 concentration. In Figure 3, an ion mobility spectrum and four mass-selected ion mobility spectra (recorded by the mass spectrometer operated in the single-ion mode) are shown under the conditions described in Figure 2. It is seen that the three ions, Cl^- , $\text{Cl}^-(\text{CHCl}_3)_1$, and $\text{Cl}^-(\text{CHCl}_3)_2$, arrive at the detector at exactly the same time and, therefore, are jointly responsible for the major peak observed at 54.0 ms in mobility spectrum 3a. In a corresponding experiment with no CHCl_3 added to the drift gas (as in spectra 1a), only the Cl^- ion was detected under the mobility peak at 34.0 ms. Clearly, the systematic increases in drift time noted in Figure 1 are caused by progressively increased clustering by reaction 2. The fact that the three ions shown in mobility spectra 3b–3d exhibit essentially identical arrival time distributions indicate that the rates of the forward and reverse clustering reactions (reaction 2) are much greater than the rates of transport for these ions through the drift tube.

Figure 3e indicates an ion labeled " $\text{Cl}^-(46)$ " that is thought to be formed by a slow reaction of formic acid with the set of

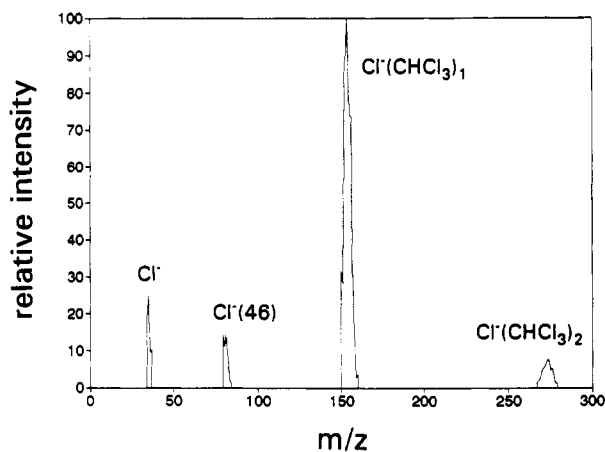


Figure 2. Mass spectra of the source-produced Cl^- ions obtained with 9.0×10^{-5} atm of CHCl_3 added to the drift gas and with the Tyndall gate continuously open. Resolution setting of the mass spectrometer is low (± 3 amu). $T = 125$ °C.

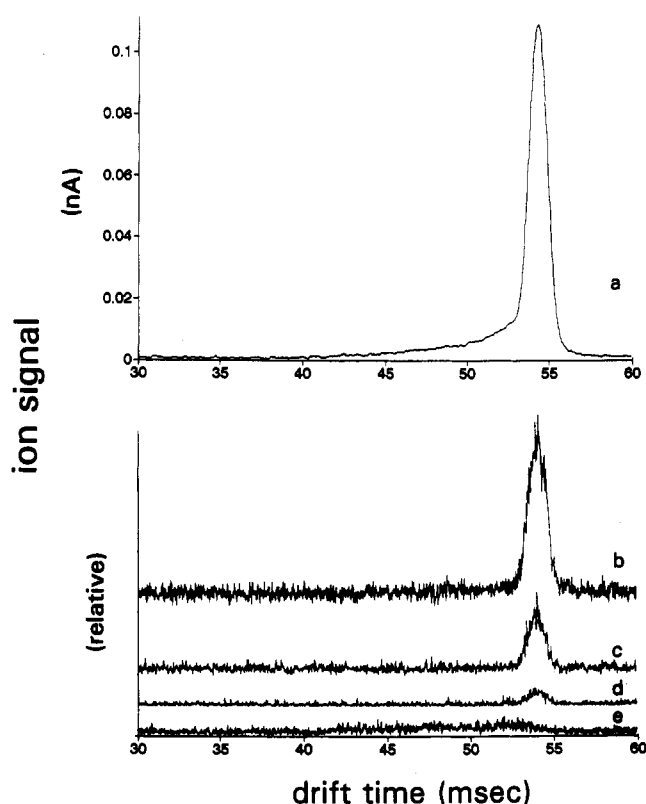


Figure 3. Ion mobility spectra of the source-produced Cl^- ions (Tyndall gate width is 0.5 ms) obtained with 9.0×10^{-5} atm of CHCl_3 added to the drift gas. Spectra have been recorded using the Faraday plate (a) and the single-ion mode of the mass spectrometer (b–e). The single ions monitored are (b) $\text{Cl}^-(\text{CHCl}_3)_1$, (c) Cl^- , (d) $\text{Cl}^-(\text{CHCl}_3)_2$, and (e) $\text{Cl}^-(46)$. $T = 125$ °C.

$\text{Cl}^-(\text{CHCl}_3)_1$ ions as they are transported through the drift region.⁹ The $\text{Cl}^-(46)$ ion has greater mobility than the $\text{Cl}^-(\text{CHCl}_3)_1$ ion packet and, therefore, arrives at the detector over a range of drift times less than 54 ms. As previously described,⁹ formic acid is thought to be formed in small amounts on the surfaces of the KIMMS instrument. It has been found that the intensity of this ion can be reduced by careful drying in the buffer gas supplies, and in the present study, the intensity of the $\text{Cl}^-(46)$ ion has been reduced to a sufficiently low level that the primary reactions of interest can be successfully studied.

Numerous measurements, of the type shown in Figure 1, were made at temperatures of 125, 100, and 75 °C using both Cl^- and Br^- as the core ions. The drift times, t_{obs} , observed at 125 and 75 °C have been plotted in Figures 4 and 5 against the

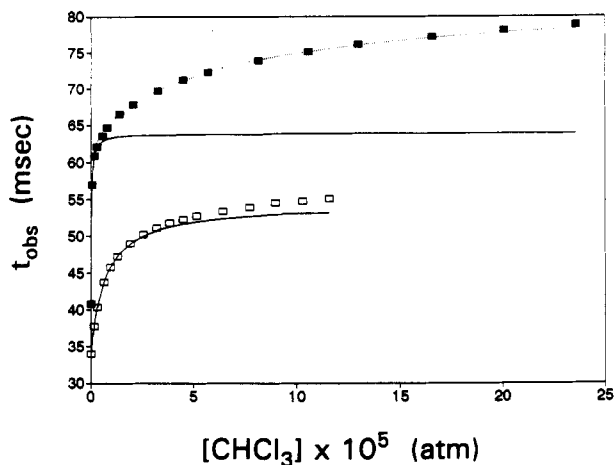


Figure 4. Observed drift times for the source-produced Cl^- ions as a function of the amount of CHCl_3 added to the drift gas. Open squares are measurements made at 125 °C. Solid squares were obtained at 75 °C. The solid and dotted curves shown are explained in the text.

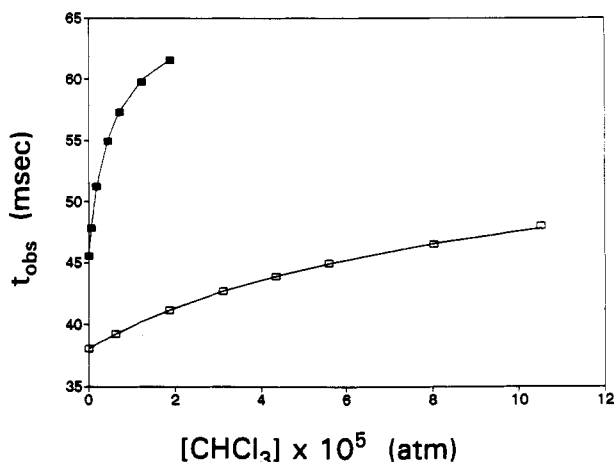


Figure 5. Observed drift times for the Br^- ion (obtained by electron capture to CF_3Br) as a function of the amount of CHCl_3 added to the drift gas. Open squares are measurements made at 125 °C. Solid squares were obtained at 75 °C. The solid curves are explained in the text.

concentration of CHCl_3 added to the drift gas. The observed drift times are expected to be related to the equilibrium constants for the clustering reactions and the mobilities of the individual cluster ions by the following general relationships:

$$t_{\text{obs}} = t_0\alpha_0 + t_1\alpha_1 + t_2\alpha_2 + \dots + t_n\alpha_n \quad (4)$$

$$\alpha_0 = 1/(1 + K_1[\text{S}] + K_1K_2[\text{S}]^2 + \dots + K_1K_2\dots K_n[\text{S}]^n) \quad (5)$$

$$\alpha_1 = K_1[\text{S}]/D \quad (6)$$

$$\alpha_2 = K_1K_2[\text{S}]^2/D \quad (7)$$

$$\alpha_i = K_1K_2\dots K_i[\text{S}]^i/D \quad (8)$$

where t_i is the drift time expected for an individual cluster ion containing i chloroform molecules, α_i is the fraction of ions under a mobility peak containing i chloroform molecules, K_i is the equilibrium constant for reaction 2 leading to the cluster ion, $\text{X}^-(\text{CHCl}_3)_i$, $[\text{S}]$ is the concentration of chloroform in the drift gas, and D is the denominator written in eq 5. Over a range of small $[\text{S}]$, where only α_0 and α_1 contribute significantly to t_{obs} , eqs 4–8 can be reduced to eq 9. In Figure 6, the mobility data

$$(t_{\text{obs}} - t_0)^{-1} = (K_1(t_1 - t_0)[\text{S}])^{-1} + (t_1 - t_0)^{-1} \quad (9)$$

for the chloride system at 125 °C (Figure 4, open squares) have been plotted in the form $(t_{\text{obs}} - t_0)^{-1}$ vs $[\text{S}]^{-1}$. In accordance with

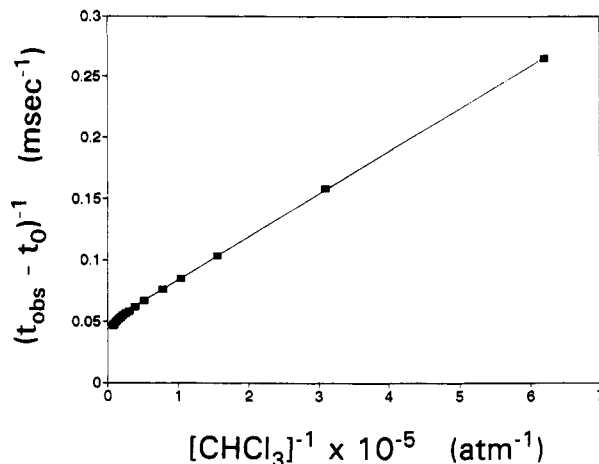


Figure 6. Mobility data obtained for the Cl^- system at 125 °C (open squares in Figure 4) plotted in the form of eq 9.

TABLE II: Summary of Results from Mobility Measurements

	temperature, °C		
	75	100	125
	$\text{Cl}^-(\text{CHCl}_3)_{0-2}$		
t_0^a	40.80	36.84	33.99
t_1	63.84	57.88	54.35
t_2	82.64		
$K_{0,0}^b$	2.725	2.820	2.883
$K_{0,1}$	1.742	1.795	1.803
$K_{0,2}$	1.346		
Ω_0^c	0.919	0.858	0.813
Ω_1	1.168	1.095	1.056
Ω_2	1.461		
K_1^d	3.7×10^6	6.1×10^5	1.41×10^5
K_2	1.43×10^4		
$\Delta H_{0,1}^e$			-18.1
$\Delta S_{0,1}^f$			-21.8
	$\text{Br}^-(\text{CHCl}_3)_{0-1}$		
t_0^a	45.55	41.24	38.04
t_1	65.97	59.83	56.31
$K_{0,0}^b$	2.445	2.523	2.548
$K_{0,1}$	1.688	1.739	1.721
Ω_0^c	0.890	0.833	0.799
Ω_1	1.185	1.111	1.087
K_1^d	1.91×10^5	4.1×10^4	1.10×10^4
$\Delta H_{0,1}^e$			-15.8
$\Delta S_{0,1}^f$			-21.1

^a Drift time, t_i , in ms of single ion $\text{X}^-(\text{CHCl}_3)_i$. ^b Reduced mobility, $K_{0,i}$, in $\text{cm}^2 \text{V}^{-1} \text{s}^{-1}$ of single ion $\text{X}^-(\text{CHCl}_3)_i$, calculated from eq 10. ^c Ion–buffer gas interaction cross section, Ω_i , in nm^2 for single ion $\text{X}^-(\text{CHCl}_3)_i$, calculated from eq 12. ^d Equilibrium constant, K_i , in atm^{-1} for the reaction $\text{X}^-(\text{CHCl}_3)_{i-1} + \text{CHCl}_3 = \text{X}^-(\text{CHCl}_3)_i$. ^e Enthalpy of $\text{X}^-(\text{CHCl}_3)_i$ formation in kcal mol^{-1} determined from van't Hoff plot in Figure 7. ^f Entropy of $\text{X}^-(\text{CHCl}_3)_i$ formation in $\text{cal deg}^{-1} \text{mol}^{-1}$ determined from van't Hoff plot in Figure 7.

eq 9, a straight line is obtained over the range of measurements where $[\text{S}]$ is relatively small ($[\text{S}]^{-1}$ is large). From the intercept of this line and from measurements of t_0 for Cl^- (33.99 ms) in the absence of added CHCl_3 , the single-ion drift time, $t_1 = 54.35$ ms, for the cluster ion, $\text{Cl}^-(\text{CHCl}_3)_1$, at 125 °C is obtained. By application of this graphical method to all six sets of measurements, t_1 values for the Cl^- and Br^- systems were determined at each of the three temperatures and are listed in Table II. Also listed are t_0 values for Cl^- and Br^- determined in the absence of added CHCl_3 . From these drift times, reduced mobilities, K_0 , for all ions were then determined from the standard relationship¹⁴

$$K_0 = (L/\bar{E}t_0)(P/760)(273/T) \quad (10)$$

where L is the length of the drift tube (23.7 cm), \bar{E} is the magnitude of the drift field (140 V cm^{-1}), P is the pressure (640 Torr), and T (K) is the temperature.

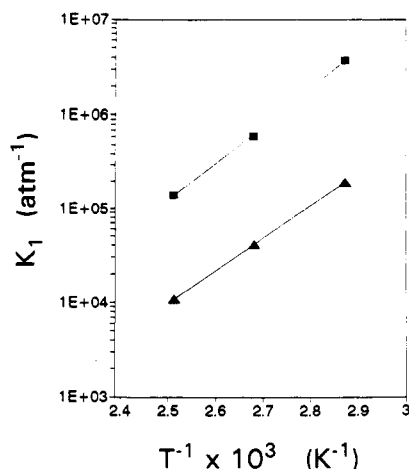


Figure 7. Equilibrium constants, K_1 , for the chloride-chloroform clustering reaction (squares) and the bromide-chloroform clustering reaction (triangles) obtained from ion mobility measurements at three temperatures, 75, 100, and 125 °C.

It is noted in Table II that the values of K_0 determined for each ion tend to increase slightly with increased temperature. This behavior suggests that the mobilities of these ions are being affected somewhat by weak chemical interactions of the ions with the drift gas (either with the major component, nitrogen, or with trace impurities, such as water). These interactions are weakened with the use of higher temperatures, leading to slightly greater K_0 values. The mobility of a given ion has previously been shown to be remarkably similar in nitrogen and argon.¹⁵ It is therefore significant to point out that the values of K_0 for Cl⁻ and Br⁻ reported in Table II are in close agreement with those previously reported in argon, 2.8 cm² V⁻¹ s⁻¹ for Cl⁻ and 2.4 cm² V⁻¹ s⁻¹ for Br⁻.¹⁵ An additional discussion of the mobility results will be provided below.

The slope of the line in Figure 6 is expected (eq 9) to be equal to $(K_1(t_1 - t_0))^{-1}$. Since the drift times, t_0 and t_1 , have been determined, the slope leads to the determination, $K_1 = 1.41 \times 10^5$ atm⁻¹, for the Cl⁻ system at 125 °C. Yamdagni and Kebarle¹⁶ have also measured K_1 for the Cl⁻-CHCl₃ system over a range of temperatures by the pulsed e-beam high-pressure mass spectrometer. Their measurement of $K_1 = 1.30 \times 10^5$ atm⁻¹ at 125 °C is in good agreement with the present measurement. By the corresponding treatment of all six data sets, K_1 values for the Cl⁻ and Br⁻ systems at 75, 100, and 125 °C were determined and are listed in Table II. In Figure 7, van't Hoff plots of the K_1 values determined for the Cl⁻ and Br⁻ systems are shown to produce straight lines, as expected. By standard treatment¹⁰ of the slopes and intercepts of these lines, the enthalpy, ΔH°_1 , and entropy, ΔS°_1 , associated with the addition of one CHCl₃ molecule to Cl⁻ or Br⁻ have been determined and are also listed in Table II. The present determinations, $\Delta H^\circ_1 = -18.1$ kcal mol⁻¹ and $\Delta S^\circ_1 = -21$ cal deg⁻¹ mol⁻¹, differ somewhat from those previously reported by Yamdagni and Kebarle,¹⁶ -15.2 kcal mol⁻¹ and -14.8 cal deg⁻¹ mol⁻¹.

The solid curves shown in Figures 4 and 5 are predictions of t_{obs} obtained by eqs 4–8 using the values of t_0 , t_1 , and K_1 determined above and with the assumption that $K_i = 0$ for all $i \geq 2$. While this assumption leads to a good fit for all of the data collected for the Br⁻ systems in Figure 5, it is clear that a good fit is observed for the Cl⁻ systems in Figure 4 only over a specific range of relatively low chloroform concentrations. For these systems, and especially for the Cl⁻ data set obtained at 75 °C, it is clear that higher order clustering is affecting t_{obs} as the concentration of chloroform is made relatively high. In order to determine t_2 and K_2 from these data, eq 11 can be used

$$W = -K_2 t_{\text{obs}} + K_2 t_2 \quad (11)$$

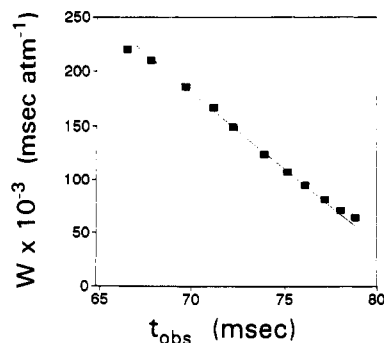


Figure 8. Mobility data obtained for the Cl⁻ system at 75 °C (solid squares in Figure 4) under conditions of relatively high CHCl₃ concentration plotted in the form of eq 11.

where

$$W = (t_{\text{obs}} + t_{\text{obs}} K_1 [S] - t_0 - t_1 K_1 [S]) / K_1 [S]^2$$

Equation 11 is derived from eqs 4–8 with the assumption that $K_i = 0$ for all $i \geq 3$ (note that all terms contributing to W are known). In Figure 8, the portion of Cl⁻ mobility data at 75 °C (Figure 4, solid squares) for which t_{obs} exceeded 65 ms has been plotted in the form W vs t_{obs} . In accordance with eq 11, a linear relationship is observed over this range of relatively high t_{obs} . Analysis of the slope of this line leads to $K_2 = 1.43 \times 10^4$ atm⁻¹ for the reaction Cl⁻(CHCl₃)₁ + CHCl₃ = Cl⁻(CHCl₃)₂ at 75 °C. To our knowledge, an equilibrium constant for this reaction has not been previously reported. Analysis of the intercept of the line in Figure 8 leads to a determination of the drift time for the cluster ion, Cl⁻(CHCl₃)₂, $t_2 = 82.64$ ms at 75 °C. The reduced mobility (eq 10) thereby determined for this ion is listed in Table II. The curve formed by the dotted line in Figure 4 is calculated from eqs 4–8 using the determinations of t_0 , t_1 , t_2 , K_1 , and K_2 described above for the Cl⁻ system at 75 °C (with the assumption that $K_i = 0$ for all $i \geq 3$). It is seen that this curve provides a good fit to almost all of the drift time measurements at 75 °C. The two data points in Figures 4 and 8 for which $t_{\text{obs}} > 77$ ms indicate the beginning of a deviation from the model calculations based on $\alpha_i = 0$ for $i \geq 3$ and, therefore, suggest that the cluster ion, Cl⁻(CHCl₃)₃, is becoming significant at 75 °C as the partial pressure of CHCl₃ reaches about 2.0×10^{-4} atm.

The Cl⁻ data sets obtained at temperatures higher than 75 °C and all three Br⁻ data sets are not treated here by eq 11 because the amount of second-order clustering achieved in these experiments was not considered to be sufficiently high as to provide accurate determinations of K_2 and t_2 .

Very few determinations of single-ion mobilities of clustered ions have previously been reported. It is therefore interesting to consider the t_i values listed in Table I in terms of the following well-established expression¹⁷ for ion mobility, K :

$$K = L/\bar{E}t_i = (3/16)(q/N)(2\pi/\mu k_B T)^{1/2}(1/\Omega) \quad (12)$$

where q is the ionic charge, N is the buffer gas number density, μ is the ion-buffer gas reduced mass, k_B is Boltzmann's constant, and Ω is the ion-buffer gas interaction cross section. By this equation, changes in drift time by the reduced mass effect, alone, can be predicted. For example, the ratio of t_i values at a given temperature for the X⁻ and X⁻(CHCl₃) ions would be 0.83 and 0.92 for the Cl⁻ and Br⁻ systems, respectively, if these ratios were determined entirely by differences in μ . Since these t_i ratios are observed to be about 0.62 and 0.68, respectively, it is clear that the major cause of decreased mobilities with formation of the first cluster ions is related to an increase in the interaction cross section rather than an increase in the reduced mass. This conclusion is also supported by mobility data of other cluster ions.¹⁵ Similarly, the main cause of the significantly increased t_2 value listed in Table II for Cl⁻(CHCl₃)₂ relative to t_1 for

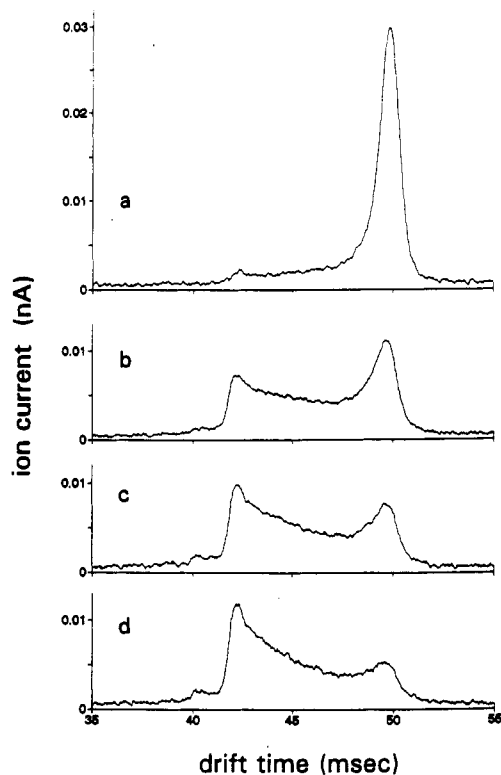


Figure 9. Kinetic ion mobility spectra of source-produced Cl^- ions with 2.22×10^{-5} atm of the clustering agent, CHCl_3 , present in the drift gas along with the following amounts of the reagent neutral, CH_3Br : (a) none, (b) 2.6×10^{12} , (c) 3.9×10^{12} , and (d) 5.3×10^{12} molecules cm^{-3} . Temperature is 125°C . Under these conditions, only 24% of the reagent ions are present as uncomplexed Cl^- ions.

$\text{Cl}^-(\text{CHCl}_3)_1$, is due to the attendant change in Ω rather than μ . The Ω values for five $\text{X}^-(\text{CHCl}_3)_i$ ions have been calculated by eq 12 from our t_i measurements at each of the three temperatures and are also listed in Table II. It is noted that the interaction cross sections of the Cl^- , $\text{Cl}^-(\text{CHCl}_3)_1$, and Br^- ions all increase by 0.24 – 0.29 nm^2 with the addition of one CHCl_3 molecule at a given temperature.

It is also noted in Table II that Ω_0 for Cl^- is slightly larger (3.3% at 75°C and 1.8% at 125°C) than that of Br^- . As in our discussion above of the K_0 values, this unexpected result suggests the significance of chemical interactions, not represented in eq 12, between some of the ions and the buffer gas (including impurities). Due to the smaller ionic radii of the Cl^- ion, this chemical interaction is expected to be greatest for it, and this apparently causes Ω_0 for Cl^- to slightly exceed that of Br^- . It is also interesting to note that Ω_1 for $\text{Cl}^-(\text{CHCl}_3)_1$ is slightly smaller than Ω_1 for $\text{Br}^-(\text{CHCl}_3)_1$. This reversal of relative Ω_i values is consistent with an expected decrease in the importance of ion–buffer gas chemical interactions following the addition of a CHCl_3 molecule to the bare Cl^- and Br^- ions.

Reactions of $\text{Cl}^-(\text{CHCl}_3)_{0-2}$ with CH_3Br and CH_3I . The chemical reactivity of a packet of ions, $\text{Cl}^-(\text{CHCl}_3)_{0-2}$, can be readily observed by the KIMMS, as illustrated in Figure 9. In Figure 9a, a mobility spectrum is shown for Cl^- ion in the presence of the clustering agent, CHCl_3 . As previously shown (Figure 3), this mobility spectrum consists primarily of a major peak at 49.5 ms that is due the simultaneous arrival of several ions of the type $\text{Cl}^-(\text{CHCl}_3)_{0-2}$. A low-intensity shoulder of this peak extending to shorter drift times is again due to the formation of the $\text{Cl}^-(46)$ ion formed from trace amounts of formic acid in the drift gas. In spectra 9b–9d, progressively greater amounts of CH_3Br have been added to the drift gas so that overall reaction 13 is made

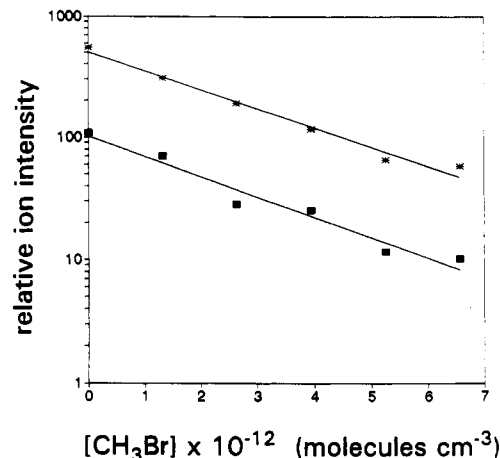


Figure 10. Mass spectrometric measurements (Tyndall gate open) of the relative intensities of the reagent ions, Cl^- (*), and $\text{Cl}^-(\text{CHCl}_3)_1$ (■), as a function of CH_3Br concentration in the drift gas. The drift gas also contains 2.22×10^{-5} atm of CHCl_3 . Temperature is 125°C .

to occur along the entire length of the drift tube. It is noted in spectra 9b–9d that as the intensity of the mobility peak at 49.5 ms is decreased by the loss of $\text{Cl}^-(\text{CHCl}_3)_{0-2}$ by reaction 13, a new component of the wave form is progressively developed that consists of an inclined plateau extending from 49.5 ms to lower arrival times and reaching a maximum at 42.0 ms. This lower end of the wave at 42 ms corresponds to the expected arrival time of the $\text{Br}^-(\text{CHCl}_3)_{0-2}$ ion packet under these conditions (see Figure 5). The fact that the bromide ion packet has shorter drift time than the chloride ion packet is due to the more extensive clustering of Cl^- at this CHCl_3 concentration.

The general shapes of the wave forms shown in Figure 9 are consistent with the occurrence of reaction 13 along the length of the drift tube. As we have previously shown,⁹ the magnitude of the overall rate constant, k_{obs} , for reaction 13 can be determined by analysis of the areas underlying the two components of each wave form. By this treatment, $k_{\text{obs}} = 7.3 \times 10^{-12}$ $\text{cm}^3 \text{ s}^{-1}$ for reaction 13 is obtained. Because of the presence of the impurity ion in these spectra (Figure 3e), k_{obs} was considered to be somewhat more accurately obtained by an alternate KIMMS method in which the mass spectrometer is used. By this approach, the Tyndall gate is operated in the continuously open mode and the diminution of the intensity of one or more MS-selected reagent ions is recorded as a function of CHCl_3 concentration in the drift gas. In Figure 10, log plots of the intensities of the Cl^- and $\text{Cl}^-(\text{CHCl}_3)_1$ ions against $[\text{CHCl}_3]$ are shown. It is expected that the slopes of either line determined by these two sets of measurements will be equal to $-k_{\text{obs}}t_d/2.3$ where t_d is the drift time of the Cl^- ion packet (t_d is determined by momentary operation of the Tyndall gate in the pulsed mode). As expected for two potential reagent ions that are coupled by fast equilibria reaction 2, the slopes of the two lines in Figure 10 are identical, each indicating $k_{\text{obs}} = 8.2 \times 10^{-12}$ $\text{cm}^3 \text{ s}^{-1}$.

Measurements of k_{obs} were made by the method illustrated in Figure 10 using four different conditions of CHCl_3 concentration. These results are plotted in Figure 11 against CHCl_3 concentration. It is seen that k_{obs} is continuously decreased as the concentration of CHCl_3 and the degree of clustering of Cl^- are increased. Under our conditions, k_{obs} is expected to be equal to the sum of the individual rate constants, k_i , for the reactions of the individual $\text{Cl}^-(\text{CHCl}_3)_i$ ions weighted by the relative abundances, α_i (eqs 5–8), for each ion. The solid curve shown in Figure 11 is a prediction for k_{obs} obtained from $K_1 = 1.41 \times 10^5$ atm^{-1} at 125°C and by assuming that the rate constants for the reactions of all cluster ions, $\text{Cl}^-(\text{CHCl}_3)_{\geq 1}$, with CH_3Br are of negligible magnitude relative to that of Cl^- . It is seen that this simple view of reaction 13 provides an adequate explanation for the dependence of k_{obs} on $[\text{CHCl}_3]$.

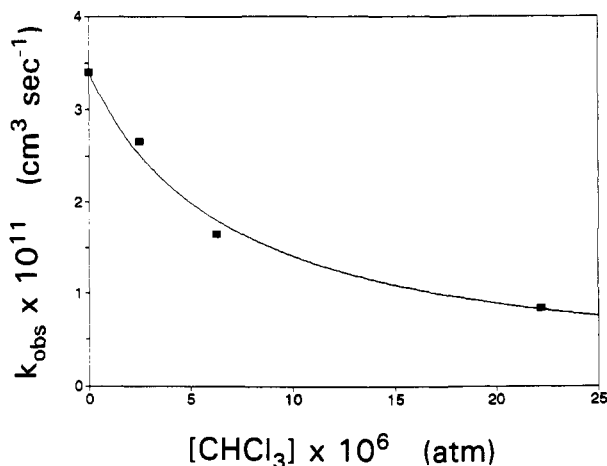
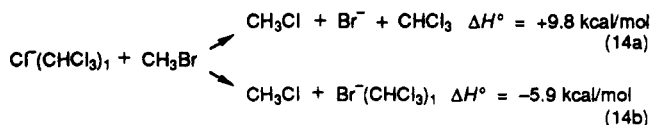


Figure 11. Rate constants observed for the reactions of $\text{Cl}^-(\text{CHCl}_3)_{0-2}$ ions with CH_3Br as a function of CHCl_3 concentration in the drift gas. Temperature is 125 °C. The solid line shown is a prediction for k_{obs} based on the assumption that only the uncomplexed Cl^- ion reacts with CH_3Br .

It is instructive to consider the lack of measurable reactivity for the $\text{Cl}^-(\text{CHCl}_3)_1$ ion in terms of the two potential elementary steps for this reaction shown in reactions 14a and 14b. The

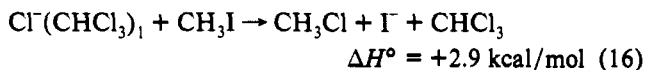


products shown in reaction 14a are those most reasonably expected if the reaction occurs by a concerted $\text{S}_{\text{N}}2$ nucleophilic displacement mechanism. As the negative charge originally centered on the Cl^- ion becomes delocalized in the transition state, the CHCl_3 molecule is envisioned to fall away from the Cl^- ion. The rate constant for reaction 14a is expected to be very small at 125 °C, however, because it is endothermic by almost 10 kcal/mol. In reaction 14b, the CHCl_3 molecule is envisioned to be clustered to the Br^- ion as products initially emerge from the transition state. Due to the additional driving force provided by the ΔH°_1 for Br^- (Table II), reaction 14b is expected to be exothermic. However, reaction 14b is not expected to be kinetically feasible for the following reason. The proton offers the only sight on the CHCl_3 molecule at which a strong interaction with a negative ion can occur, and this interaction will be strong only if the negative charge of the anion is localized.¹⁸ If reaction 14b is envisioned to occur by the $\text{S}_{\text{N}}2$ mechanism, migration of the CHCl_3 molecule along the length of the concerted transition state would be required since the CHCl_3 molecule cannot effectively "bridge" the transition state by simultaneous interactions at two sights. In the transition state, the negative charge is expected to be spread over its length. Significant weakening of the interaction between CHCl_3 and the transition state would therefore be expected, and this would greatly increase the height of the transition-state barrier, thereby preventing motion along this reaction coordinate. In a previous study of the $\text{S}_{\text{N}}2$ reactions of solvated ions, little or no support for a solvent-transfer mechanism, such as in reaction 14b, was also found.¹⁹

Kinetic measurements have also been made here for the reactions of CH_3I with a selected set of $\text{Cl}^-(\text{CHCl}_3)_i$ ions. In the absence of CHCl_3 in the drift gas, a rate constant for reaction 15 of $2.2 \times 10^{-10} \text{ cm}^3 \text{ s}^{-1}$ at 125 °C was observed. (Bierbaum



*et al.*²⁰ report $k = 2.1 \times 10^{-10} \text{ cm}^3 \text{ s}^{-1}$ for this reaction at 25 °C in 1 Torr of helium buffer gas.) With $2.21 \times 10^{-5} \text{ atm}$ of CHCl_3 added to the drift gas, a lower rate constant, $k_{\text{obs}} = 4.8 \times 10^{-11} \text{ cm}^3 \text{ s}^{-1}$, was observed. The magnitude of rate constant depression caused by CHCl_3 in this case (0.22) is again consistent with a simple model in which only the unclustered Cl^- ion is envisioned to contribute to k_{obs} (by eq 5, $\alpha_0 = 0.24$). Therefore, it is concluded that the rate constant for the slightly endothermic reaction 16 is of negligible magnitude relative to that of reaction 15.



Conclusions

It has been shown here that equilibrium constants for the successive formation of small cluster ions and that rate constants for the reactions of sets of equilibrated cluster ions with another reagent molecule can be determined in an atmospheric pressure buffer gas by ion mobility measurements. Because relatively high partial pressures of a clustering agent can be attained in an atmospheric pressure buffer gas, the technique described here is expected to be particularly useful for the study of either weakly bound cluster ions or strongly bound cluster ions at high temperature.

Acknowledgment. This work was supported by the Montana/EPSCoR II Program of the National Science Foundation (Grant R11-8921978) and by the Chemical Analysis Division of the National Science Foundation (Grant CHE-9211615).

References and Notes

- (1) Matsuoka, S.; Nakamura, H. *J. Chem. Phys.* **1988**, *89*, 5663–5669.
- (2) Matsuoka, S.; Ikesoe, Y. *J. Phys. Chem.* **1988**, *92*, 1126–1133.
- (3) Collins, C. B.; Lee, F. W. *J. Chem. Phys.* **1978**, *68*, 1391–1401.
- (4) Collins, C. B.; Lee, F. W. *J. Chem. Phys.* **1979**, *71*, 184–191.
- (5) Collins, C. B.; Lee, F. W. *J. Chem. Phys.* **1980**, *72*, 5381–5389.
- (6) Cacace, F. *Science* **1990**, *250*, 392–399.
- (7) Collins, C. B.; Lee, F. W.; Tepfenhart, W. M.; Stevefelt, J. *J. Chem. Phys.* **1983**, *78*, 6079–6090.
- (8) Speranza, M. *Mass Spectrom. Rev.* **1992**, *11*, 73–117.
- (9) Giles, K.; Grimsrud, E. *J. Phys. Chem.* **1992**, *96*, 6680–6687.
- (10) Kebarle, P. *Annu. Rev. Phys. Chem.* **1977**, *28*, 445–476.
- (11) Castleman, A. W.; Keese, R. G. *Chem. Rev.* **1986**, *86*, 589–618.
- (12) Zook, D. R.; Grimsrud, E. P. *J. Phys. Chem.* **1988**, *92*, 6374–6379.
- (13) Zook, D. R.; Grimsrud, E. P. *J. Am. Soc. Mass Spectrom.* **1991**, *2*, 232–239.
- (14) Mason, E. A.; McDaniel, E. W. *Transport Properties of Ions in Gases*; John Wiley & Sons: New York, 1988; p 5.
- (15) Ellis, H. W.; McDaniel, E. W.; Albritton, D. L.; Viehland, L. A.; Lin, S. L.; Mason, E. A. *Atomic Data Nuclear Data Tables* **1978**, *22*, 179–217.
- (16) Yamdagni, R.; Kebarle, P. *J. Am. Chem. Soc.* **1971**, *93*, 7139–7143.
- (17) Revercomb, H. E.; Mason, E. A. *Anal. Chem.* **1975**, *47*, 970–983.
- (18) Magnera, T. F.; Caldwell, G.; Sunner, J.; Ikuta, S.; Kebarle, P. *J. Am. Chem. Soc.* **1984**, *106*, 6140.
- (19) Henchman, M.; Paulson, J. F.; Hierl, P. M. *J. Am. Chem. Soc.* **1983**, *105*, 5509.
- (20) Bierbaum, V. M.; Grabowski, J. J.; Depuy, C. H. *J. Phys. Chem.* **1984**, *88*, 1389.